

# Heterobuckybowls: A Theoretical Study on the Structure, Bowl-to-Bowl Inversion Barrier, Bond Length Alternation, Structure-Inversion Barrier Relationship, Stability, and Synthetic Feasibility<sup>†</sup>

U. Deva Priyakumar and G. Narahari Sastry\*

Department of Chemistry, Pondicherry University, Pondicherry 605 014, India

gnsastry@yahoo.com

Received May 21, 2001

Hybrid density functional theory (DFT) calculations at the B3LYP/cc-pVDZ level have been performed on a series of heterobuckybowls, **3X**, C<sub>18</sub>X<sub>3</sub>H<sub>6</sub> (X = O, NH, CH<sub>2</sub>, BH, S, PH, PH<sub>3</sub>, Si, SiH<sub>2</sub>, and AlH). The minimum energy conformations and the transition states for bowl-to-bowl inversion, where the geometry is bowl shaped, are computed and characterized by frequency calculations. The geometries of heterotrindenes, **2X**, C<sub>12</sub>X<sub>3</sub>H<sub>6</sub> (X = O, NH, CH<sub>2</sub>, BH, S, PH, PH<sub>3</sub>, Si, SiH<sub>2</sub>, and AlH), were obtained, and the bond length alternation ( $\Delta$ ) in the central benzenoid ring shows remarkable sensitivity as a function of substituent with a wide range of fluctuations (−0.014 to +0.092 Å). The  $\Delta$  computed in **2BH** was found to be comparable with the highest bond alternation reported to date in benzenoid frameworks. The inversion dynamics of these heterobowls and their bowl depths were fit to a mixed quartic/quadratic function. The size of the heteroatom seems to exclusively control the bowl depth and rigidity as well as the synthetic feasibility. In contrast, the bond length alternation seems to be controlled by electronic factors and not by the size of the substituted atom either in trindenes or in heterosumanenes. The thermodynamic stability of this class of compounds is very much comparable with trithiasumanene (**3S**), which has been synthesized recently. The chemical hardness ( $\eta$ ) was measured to assess the stability of the heterosumanenes. The strain energy buildup in a sequential ring closure strategy along two synthetic routes, namely a triphenylene route and a trindene route, were explored, and the trindene route was found to be highly favorable for making such compounds compared to the triphenylene route. However, in both routes the ease of the synthetic feasibility increases as the size of the heteroatom increases.

## 1. Introduction

The discovery of fullerenes stimulated contemporary chemistry researchers to investigate and unravel the unique structural, electronic, optical, biological, magnetic, and other properties of this potentially promising class of compounds.<sup>1,2</sup> Although the attempts to achieve the synthesis of C<sub>60</sub> by rational means are yet to be successful, these attempts have opened an exciting area in the synthetic organic chemistry, in the form of buckybowl chemistry.<sup>3–7</sup> A large number of interesting bowl-like moieties, which form a part of C<sub>60</sub>, have been synthesized and were shown to exhibit novel structural, chemical, and

physical properties.<sup>8–12</sup> Computations played a pivotal role in understanding and modeling the novel properties of buckybowls.<sup>13–20</sup> In fullerene chemistry, heterohedral fullerenes, where one or more skeletal C atoms are

<sup>†</sup> Dedicated to Professor J. Subramanian on the occasion of his 60th birthday.

(1) Kroto, H. W.; Heath, J. R.; O'Brian, S. C.; Curl, R. F.; Smalley, R. E. *Nature* **1985**, *318*, 162.

(2) Hirsch, A. *The Chemistry of the Fullerenes*; Georg Thieme Verlag: Stuttgart, New York, 1994.

(3) Faust, R. *Angew. Chem., Int. Ed. Engl.* **1995**, *34*, 1429.

(4) (a) Rabideau, P. W.; Sygula, A. *Acc. Chem. Res.* **1996**, *29*, 235.

(b) Rabideau, P. W.; Sygula, A. In *Advances in theoretically interesting molecules*; Thummel, R. P., Ed.; JAI Press: Greenwich, CT, 1995; Vol. 3, pp 1–36.

(5) (a) Mehta, G.; Rao, H. S. P. *Tetrahedron* **1998**, *54*, 13325. (b) Mehta, G.; Rao, H. S. P. In *Advances in Strain in Organic Chemistry*; Halton, B., Ed.; JAI Press: London, 1997; Vol. 6, pp 139–187.

(6) Mehta, G.; Panda, G. *Proc. Indian Natl. Sci. Acad., Part A* **1998**, *64*, 587.

(7) (a) Scott, L. T. *Pure Appl. Chem.* **1996**, *68*, 291. (b) Scott, L. T.; Bronstein, H. E.; Preda, D. V.; Ansems, R. B. M.; Bratcher, M. S.; Hagen, S. *Pure Appl. Chem.* **1999**, *71*, 209.

(8) (a) Barth, W. E.; Lawton, R. G. *J. Am. Chem. Soc.* **1966**, *88*, 380. (b) Barth, W. E.; Lawton, R. G. *J. Am. Chem. Soc.* **1971**, *93*, 1730.

(9) (a) Ansems, R. B. M.; Scott, L. T. *J. Am. Chem. Soc.* **2000**, *122*, 2719. (b) Hagen, S.; Bratcher, M. S.; Erickson, M. S.; Zimmermann, G.; Scott, L. T. *Angew. Chem., Int. Ed. Engl.* **1997**, *36*, 406. (c) Mehta, G.; Panda, G. *Chem. Commun.* **1997**, 2081. (d) Clayton, M. D.; Rabideau, P. W. *Tetrahedron Lett.* **1997**, *38*, 741. (e) Clayton, M. D.; Marcinow, Z.; Rabideau, P. W. *J. Org. Chem.* **1996**, *61*, 6052. (f) Scott, L. T.; Bratcher, M. S.; Hagen, S. *J. Am. Chem. Soc.* **1996**, *118*, 8743.

(g) Rabideau, P. W.; Abdourazak, A. H.; Folsom, H. E.; Marcinow, Z.; Sygula, A.; Sygula, R. *J. Am. Chem. Soc.* **1994**, *116*, 7891. (10) (a) Scott, L. T.; Hashemi, M. M.; Bratcher, M. S. *J. Am. Chem. Soc.* **1992**, *114*, 1920. (b) Borchardt, A.; Fuchicello, A.; Kilway, K. V.; Baldrige, K. K.; Siegel, J. S. *J. Am. Chem. Soc.* **1992**, *114*, 1921.

(11) (a) Sygula, A.; Rabideau, P. W. *J. Am. Chem. Soc.* **1999**, *121*, 7800. (b) Abdourazak, A. H.; Sygula, A.; Rabideau, P. W. *J. Am. Chem. Soc.* **1993**, *115*, 3010. (c) Sygula, A.; Abdourazak, A. H.; Rabideau, P. W. *J. Am. Chem. Soc.* **1996**, *118*, 339.

(12) Seiders, T. J.; Baldrige, K. K.; Siegel, J. S. *J. Am. Chem. Soc.* **1996**, *118*, 2754.

(13) Sastry, G. N.; Jemmis, E. D.; Mehta, G.; Shah, S. R. *J. Chem. Soc., Perkin Trans. 2* **1993**, 1867.

(14) Biedermann, P. U.; Pogodin, S.; Agranat, I. *J. Org. Chem.* **1999**, *64*, 3655.

(15) Baldrige, K. K.; Siegel, J. S. *Theor. Chem. Acc.* **1997**, *97*, 67.

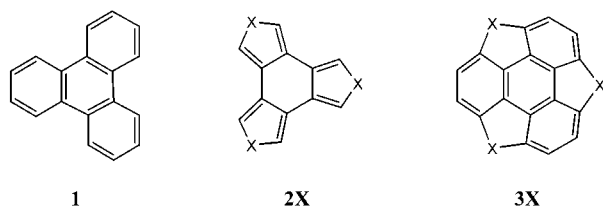
(16) (a) Baldrige, K. K.; Siegel, J. S. *J. Am. Chem. Soc.* **1999**, *121*, 5332. (b) Seiders, T. J.; Baldrige, K. K.; Elliott, E. L.; Grube, G. H.; Siegel, J. S. *J. Am. Chem. Soc.* **1999**, *121*, 7439.

(17) Martin, J. M. L. *Chem. Phys. Lett.* **1996**, *262*, 97.

(18) Sygula, A.; Rabideau, P. W. *THEOCHEM* **1995**, *333*, 215.

(19) Schulman, J. M.; Disch, R. L. *J. Comput. Chem.* **1998**, *19*, 189.

Scheme 1



X = O, NH, CH<sub>2</sub>, BH, S, PH, PH<sub>3</sub>, Si, SiH<sub>2</sub>, AlH

replaced by heteroatoms, such as B, Si, and N, have attracted considerable attention, and these dopyballs are considered to modulate the superconducting, electrical, and redox properties of fullerenes.<sup>21,22</sup>

Recently, Otsubo et al. reported the synthesis of **3S**, triphenyleno[1,12-*bcd*:4,5-*b'c'd'*:8,9-*b''c''d''*]trithiophene, the first heterobuckybowl.<sup>23</sup> These bowl-shaped heteroaromatics were conceived to exhibit novel physicochemical properties such as organic conducting materials.<sup>23,24</sup> The corresponding hydrocarbon moiety, where the three S groups replaced by CH<sub>2</sub>, sumanene (**3CH<sub>2</sub>**), C<sub>21</sub>H<sub>12</sub>, was recognized as a key structural motif of C<sub>60</sub> similar to corannulene (Scheme 1).<sup>25,26</sup> Siegel and co-workers reported that a double well potential, given by mixed quartic/quadratic function, seems to model the inversion dynamics in a series of corannulene derivatives.<sup>27,28</sup> Replacement of skeletal carbon atoms by iso-electronic substituents was shown to be the most effective way of modulating the curvature, bowl-to-bowl inversion barrier, and the consequent physicochemical properties.<sup>29–32</sup> In this context, it is interesting to test the applicability of the structure–energy correlations in the inversion dynamics of heterobuckybowls.

Requirements for introducing bond alternation in benzene have been a subject of interest for a long time.<sup>33,34</sup>

The significant bond alternation that exists in triphenylene,<sup>34c,35</sup> trindene, and C<sub>60</sub><sup>36</sup> prompted us to critically analyze the bond length alternation in this class of compounds. Therefore, an examination of bond alternation in trindenenes and heterosumanenes, in the flat as well as in the bowl form as a function of substituent, is interesting in its own right (Scheme 1). The heterosumanenes have 18- $\pi$  electrons and 18-sp<sup>2</sup> centers for X = CH<sub>2</sub>, PH<sub>3</sub>, and SiH<sub>2</sub>; 18- $\pi$  electrons and 21-sp<sup>2</sup> centers for X = BH, Al, and Si; and 24- $\pi$  electrons and 21-sp<sup>2</sup> centers for X = NH, PH, O, and S. “Annulene – within an annulene”, where both the rim and hub attain the aromatic Huckel count, has been evoked to account for the stability in fused polycyclic aromatic systems.<sup>37</sup> Thus, according to this model, the heterobuckybowls are stable only for X = NH, PH, O, and S with a 6 $\pi$  hub and an 18 $\pi$  rim electron count. Computational quantum chemistry provides the practicing chemists an unprecedented opportunity to obtain structure, energy, and other physicochemical properties of potentially interesting class of molecules where no experimental data are available. Heteroaromatics in general and nonplanar heteroaromatics in particular could potentially exhibit novel conducting properties and thus form a new class of compounds,<sup>24</sup> and the interplay between theory and experiment is essential for its growth. C<sub>18</sub>-triphenylene and C<sub>15</sub>-trindene are the two planar C<sub>3</sub>-symmetric hydrocarbons, which map on the C<sub>60</sub> surface in addition to the planar benzene and 6-radialene.<sup>13</sup> Both of them are accessible in quantities and are amenable to structural functionalization.<sup>5,6,38</sup> The synthetic feasibility of these heterobuckybowls is explored through two possible routes: namely the trindene route and the triphenylene route.<sup>31a</sup>

In this study, we analyze in detail the effect of replacing the three unique CH<sub>2</sub> groups in sumanene (**3CH<sub>2</sub>**) by X = O, NH, BH, S, PH, PH<sub>3</sub>, Si, SiH<sub>2</sub>, and AlH on the geometry, curvature, inversion barrier, and feasibility of their syntheses. The following points are addressed in the present study: (a) the relation between the size of the heteroatom and the bowl depth, rigidity and inversion barrier, (b) the bond length alternation in this class of compounds, (c) the structure–energy correlation, (d) the stability through homodesmotic equations and hardness, and (e) the synthetic feasibility of heterosumanenes along two distinct pathways.

## 2. Methodology

The planar D<sub>3h</sub> structures (C<sub>3h</sub> for X = PH<sub>3</sub>) of all the heterosumanenes (**3X**) considered in this study were optimized within the symmetry constraints using the hybrid density functional B3LYP<sup>39</sup> method with the cc-pVDZ basis set.<sup>40</sup> Frequency calculations were done at the same level to ascer-

(20) (a) Dinadayalane, T. C.; Priyakumar, U. D.; Sastry, G. N. *THEOCHEM* **2001**, 543, 1. (b) Dinadayalane, T. C.; Sastry, G. N. *THEOCHEM*, submitted.

(21) (a) Chen, Z.; Zhao, X.; Tang, A. *J. Phys. Chem. A* **1999**, 103, 10961. (b) Ray, C.; Pellarin, M.; Lerme, J. L.; Vialle, J. L.; Broeyer, M.; Blase, X.; Melinon, P.; Keghelian, P.; Perez, A. *Phys. Rev. Lett.* **1998**, 80, 5365. (c) Hasharoni, K.; Bellavia-Lund, C.; Keshavarz-K, M.; Srdanov, G.; Wudl, F. *J. Am. Chem. Soc.* **1997**, 119, 11128.

(22) (a) Billas, I. M. L.; Massobrio, C.; Boero, M.; Parrinello, M.; Branz, W.; Tast, F.; Malinowski, N.; Heinebrodt, M.; Martin, T. P. *J. Chem. Phys.* **1999**, 111, 6787. (b) Chen, Z.; Jiao, H.; Hirsch, A.; Thiel, W. *Chem. Phys. Lett.* **2000**, 329, 47. (c) Chistyakov, A. C.; Stankevich, I. V. *Inorg. Chim. Acta* **1998**, 280, 219. (d) Knapfer, M.; Pichler, T.; Golden, M. S.; Fink, J. *Proc. Electrochem. Soc.* **1998**, 98, 673.

(23) Imamura, K.; Takimiya, K.; Aso, Y.; Otsubo, T. *Chem. Commun.* **1999**, 1859.

(24) (a) Otsubo, T. *Synlett* **1997**, 544. (b) Caronna, T.; Sinisi, R.; Catellani, M.; Malpezzi, L.; Meille, S. V.; Mele, A. *Chem. Commun.* **2000**, 1139.

(25) Mehta, G.; Shah, S. R.; Ravikumar, K. *J. Chem. Soc., Chem. Commun.* **1993**, 1006.

(26) Priyakumar, U. D.; Sastry, G. N. *J. Phys. Chem. A* **2001**, 105, 4488.

(27) (a) Burgi, H.-B.; Dubler-Steudle, K. C. *J. Am. Chem. Soc.* **1988**, 110, 4953. (b) Burgi, H.-B.; Dunitz, J. D. *Structure Correlation*; VCH: Weinheim, New York, 1994. (c) Burgi, H.-B. *Acta Crystallogr.* **1998**, A54, 873.

(28) Seiders, T. J.; Baldrige, K. K.; Grube, G. H.; Siegel, J. S. *J. Am. Chem. Soc.* **2001**, 123, 517.

(29) Sastry, G. N.; Rao, H. S. P.; Bednarek, P.; Priyakumar, U. D. *Chem. Commun.* **2000**, 843.

(30) Sastry, G. N.; Priyakumar, U. D. *J. Chem. Soc., Perkin Trans. 2* **2001**, 30.

(31) (a) Priyakumar, U. D.; Sastry, G. N. *Tetrahedron Lett.* **2001**, 42, 1379. (b) Priyakumar, U. D.; Sastry, G. N. *J. Mol. Graphics Mod.* **2001**, 19, 266.

(32) Delaere, D.; Nguyen, M. T.; Vanquickenborne, L. G. *Chem. Phys. Lett.* **2001**, 333, 103.

(33) Mills, W. H.; Nixon, I. G. *J. Chem. Soc.* **1930**, 2510.

(34) (a) Siegel, J. S. *Angew. Chem., Int. Ed. Engl.* **1994**, 33, 1721. (b) Lu, Y.; Lemal, D. M.; Jasinski, J. P. *J. Am. Chem. Soc.* **2000**, 122, 2440. (c) Baldrige, K. K.; Siegel, J. S. *J. Am. Chem. Soc.* **1992**, 114, 9583. (d) Frank, N. L.; Baldrige, K. K.; Siegel, J. S. *J. Am. Chem. Soc.* **1995**, 117, 2102. (e) Burgi, H.-B.; Baldrige, K. K.; Hardcastle, K.; Frank, N. L.; Gantzel, P.; Siegel, J. S.; Ziller, J. *Angew. Chem., Int. Ed. Engl.* **1995**, 34, 1454. (f) Shaik, S.; Shurki, A.; Danovich, D.; Hiberty, P. C. *Chem. Rev.* **2001**, 101, 1501.

(35) Filippini, G. *J. Mol. Struct.* **1985**, 130, 117.

(36) Hedberg, K.; Hedberg, L.; Bethune, D. S.; Brown, C. A.; Dorn, H. C.; Johnson, R. D.; Vries, M. D. *Science* **1991**, 312, 410.

(37) Ayalon, A.; Rabinovitz, M.; Cheng, P.-C.; Scott, L. T. *Angew. Chem., Int. Ed. Engl.* **1992**, 31, 1636.

(38) (a) Dehmloew, E. V.; Kelle, T. *Synth. Commun.* **1997**, 27, 2021. (b) Ferrier, R. J.; Holden, S. G.; Gladkikh, O. *J. Chem. Soc., Perkin Trans. 1* **2000**, 3505.

tain the nature of the stationary points. The  $D_{3h}$  structures of **3O**, **3NH**, **3CH<sub>2</sub>**, **3BH**, and **3S** were characterized as transition states, corresponding to the bowl-to-bowl inversion process. However, the  $C_{3h}$  structure of **3PH<sub>3</sub>** and the  $D_{3h}$  structures of **3Si**, **3SiH<sub>2</sub>**, and **3AlH** were characterized as minima on their respective potential energy surfaces.<sup>41</sup> For X = O, NH, CH<sub>2</sub>, BH, S, and PH, the minimum energy bowl structures were obtained by following the normal modes corresponding to the respective imaginary frequencies. The resultant bowl structures with  $C_{3v}$  symmetry have been characterized as the minima by frequency calculations in all cases. All the  $D_{3h}$  forms of heterotrindenes (**2X**), C<sub>12</sub>X<sub>3</sub>H<sub>6</sub>, were also optimized, and the stationary points were characterized by frequency calculations at the B3LYP/cc-pVDZ level. The planar structures of **2X** were characterized as minima except for **2PH**, **2Si**, and **2AlH**, which were found to be third-order saddle points.<sup>42</sup> B3LYP/cc-pVDZ level has been proven to be a reliable method for predicting the equilibrium geometries, inversion barriers and harmonic frequencies of buckybowls especially when post-SCF methods are not practical for molecules of this size.<sup>14–17,26</sup> In the synthetic strategies toward heterosumanenes, all the species were optimized without any symmetric constraints and characterized as minima at the MNDO level.<sup>43</sup> This is followed by single-point calculations at the B3LYP/cc-pVDZ level on all the MNDO-optimized points in both the synthetic routes. All the calculations were done using the Gaussian 94 suite of programs.<sup>44</sup> The nature of the normal modes were examined using the MOPLOT graphical interface program.<sup>45</sup>

### 3. Results and Discussion

**3.1. Equilibrium Geometries.** The equilibrium geometries and the bond length alternations ( $\Delta$ ) in the trindenes (**2X**) will be discussed first. The salient structural parameters, with special attention to the bond length alternation in the central benzenoid ring, of the heterosumanenes (**3X**) as well as the bowl-to-bowl inversion transition states (**3X'**), are given next.

**3.1.1. Trindenes, 2X.** Trindenes may be viewed as three substituted cyclopentadienes annulated to a benzene ring maintaining the 3-fold axis. These cyclopentadienes can be classified into three types based on the electron count: (i) 6 $\pi$ -systems, **2O**, **2NH**, **2S**, **2PH**; (ii) conjugated 4 $\pi$ -systems, **2BH**, **2Si**, **2AlH**; and (iii) unconjugated 4 $\pi$ -systems, **2CH<sub>2</sub>**, **2PH<sub>3</sub>**, **2SiH<sub>2</sub>**.

(39) (a) Becke, A. D. *J. Chem. Phys.* **1993**, *98*, 5648. (b) Lee, C.; Yang, W.; Parr, R. G. *Phys. Rev. B* **1988**, *37*, 785.

(40) Woon, D. E.; Dunning, Jr., T. H. *J. Chem. Phys.* **1993**, *98*, 1358.

(41) **3PH**, bowl is virtually flat with a tiny bowl depth of 0.118 Å. Frequency analysis of  $D_{3h}$  flat structure shows three imaginary frequencies each corresponding to the P–H out-of-plane vibrations. Numerous attempts to locate the real bowl-to-bowl inversion transition state are futile. The fourth normal mode, which actually corresponds to the bowl-to-bowl inversion, has a real frequency measuring 56.7 cm<sup>−1</sup> at the B3LYP/cc-pVDZ level. Therefore for all practical purposes, **3PH** may be considered to have a planar skeleton. For **3PH**, another minima with  $C_s$  symmetry is obtained but it is virtually identical in energy compared to the bowl (see also ref 22), since we are interested in bowl shaped molecules, only the  $C_{3v}$  structure is considered.

(42) The  $D_{3h}$  structure of **2PH**, which shows three imaginary frequencies (620i, 616i, and 616i), was optimized with  $C_{3v}$  symmetry and showed significant stabilization, which is mainly due to the pyramidalization at the P center. However, the  $D_{3h}$  structures of **2Si** and **2AlH** have three very small imaginary frequencies around 50i, and thus, these are ignored and further optimizations were not done.

(43) Dewar, M. J. S.; Thiel, W. *J. Am. Chem. Soc.* **1977**, *99*, 4899.

(44) Gaussian 94: Frisch, M. J.; Trucks, G. W.; Schlegel, H. B.; Gill, P. M. W.; Johnson, B. G.; Robb, M. A.; Cheeseman, J. R.; Keith, T.; Petersson, G. A.; Montgomery, J. A.; Ragavachari, K.; Al-Laham, M. A.; Zakrzewski, V. G.; Ortiz, J. V.; Foresman, J. B.; Cioslowski, J.; Stefanov, B. B.; Nanayakkara, A.; Challacombe, M.; Peng, C. Y.; Ayala, P. Y.; Chen, W.; Wong, M. W.; Andres, J. L.; Replogle, E. S.; Gomperts, R.; Martin, R. L.; Fox, D. J.; Binkley, J. S.; Defrees, D. J.; Baker, J.; Stewart, J. P.; Head-Gordon, M.; Gonzalez, C.; Pople, J. A. Gaussian, Inc., Pittsburgh, PA, 1995.

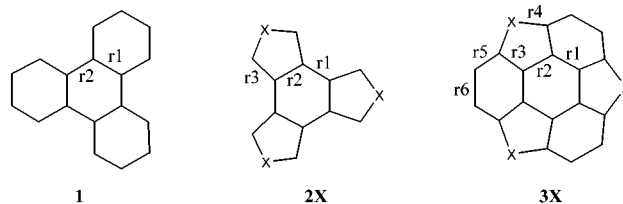
(45) Bally, T.; Albrecht, B.; Matzinger, S.; Sastry, G. M. Moplot 3.2, University of Fribourg, 1997.

**Table 1. Principal Bond Lengths and the Bond Length Alternations ( $\Delta$ ) in the Central Six-Membered Ring of the Heterotrindenes (**2X**) and Triphenylene (**1**) Obtained at the B3LYP/cc-pVDZ Level (the Experimental Bond Lengths for C<sub>60</sub>, Triphenylene (**1**), and Corannulene Are Also Given)**

structure	point group	$r_1$ (Å)	$r_2$ (Å)	$r_3$ (Å)	$\Delta^a$
C <sub>60</sub>	I <sub>h</sub>	1.401 <sup>b</sup>	1.458 <sup>b</sup>		0.057
<b>1</b>	$D_{3h}$	1.423	1.469		0.046
		(1.411) <sup>c</sup>	(1.470) <sup>c</sup>		(0.059)
corannulene	$C_{5v}$	1.410 <sup>d</sup>	1.408 <sup>d</sup>		−0.002
<b>2O</b>	$D_{3h}$	1.454	1.454	1.369	0.000
<b>2NH</b>	$D_{3h}$	1.452	1.446	1.388	−0.006
<b>2CH<sub>2</sub></b>	$D_{3h}$	1.462	1.489	1.358	0.027
<b>2BH</b>	$D_{3h}$	1.393	1.485	1.420	0.092
<b>2S</b>	$D_{3h}$	1.463	1.449	1.377	−0.014
<b>2PH</b>	$C_{3v}$	1.470	1.481	1.366	0.011
<b>2PH'</b>	$D_{3h}$	1.462	1.446	1.402	−0.016
<b>2PH<sub>3</sub></b>	$C_{3h}$	1.472	1.501	1.350	0.029
				(1.356)	
<b>2Si</b>	$D_{3h}$	1.467	1.528	1.362	0.061
<b>2SiH<sub>2</sub></b>	$D_{3h}$	1.480	1.512	1.361	0.032
<b>2AlH</b>	$D_{3h}$	1.489	1.538	1.365	0.049

<sup>a</sup>  $\Delta = r_2 - r_1$  is the bond alternation in the central six-membered ring. <sup>b</sup> The experimental bond lengths for C<sub>60</sub> are taken from ref 36. <sup>c</sup> The experimental bond lengths for triphenylene (**1**) are taken from ref 35; here, the planar structure is considered. <sup>d</sup> The experimental bond lengths for corannulene are taken from ref 54.

**Scheme 2**



The important skeletal parameters and the bond length alternations ( $\Delta$ ) in the central six-membered ring of the substituted trindenes **2X** (X = O, NH, CH<sub>2</sub>, BH, S, PH, PH<sub>3</sub>, Si, SiH<sub>2</sub>, and AlH) obtained at the B3LYP/cc-pVDZ level are given in Table 1. Scheme 2 illustrates the notations used. Annulation to benzene ring reduces its symmetry; the extent of localization of the double bonds is represented by bond length alternation ( $\Delta$ ), which is the difference between the bond lengths;  $\Delta$  is taken as  $r_2 - r_1$  (Scheme 2) uniformly for all the structures considered here.<sup>33,34</sup> Very low bond alternation is exhibited for **2O**, **2NH**, **2S**, and **2PH** where the augmented five-membered rings are aromatic. This is in sharp contrast to the situation in triphenylene (**1**),<sup>34c,35</sup> which exhibits significant bond alternation. When the augmented five-membered rings are nonaromatic, i.e., when X = CH<sub>2</sub>, PH<sub>3</sub>, and SiH<sub>2</sub>, greater bond alternation resulted. The highest bond alternation is seen in cases where the five-membered rings are conjugated 4 $\pi$  systems, when X = BH, Si, and AlH. Thus, the aromaticity of the augmented five-membered ring critically controls the bond alternation in the central six-membered ring of the heterotrindenes (Figure 1). A maximum  $\Delta$  value of 0.092 Å is observed for **2BH**, which is similar to the ever observed high alternation of 0.091 Å in triannulated benzene-type systems.<sup>34d,e</sup> In none of the cases is  $r_1$  or  $r_2$  close to the aromatic bond length except in **2BH**, where  $r_1$  is 1.393.<sup>46</sup> These results indicate that the electronic factors are chiefly responsible for bond length alternation.

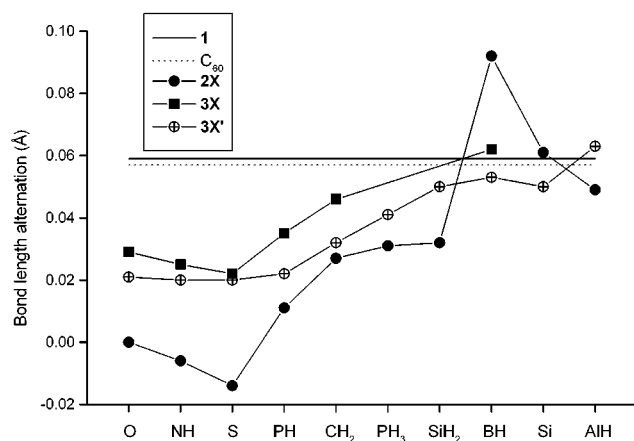


**Figure 1.** Plot of bond length alternation ( $\Delta = r_2 - r_1$ , Scheme 2) in the central six-membered rings of the heterotrindenes (**2X**) and bowl and flat forms of heterosumanenes (**3X** and **3X'**) as a function of the substituent. The substituents are grouped according to their contribution to  $\pi$ -conjugation and electron count. (Note that size was taken as a criterion to arrange X's in other places.) The  $\Delta$  in  $C_{60}$  and triphenylene (**1**) are given for comparison.

**3.1.2. Heterosumanenes, 3X.** The principal geometric parameters and the bond length alternations in the hub and rim of the minimum energy structures (**3X**) and the corresponding transition-state structures (**3X'**) of all the heterosumanenes obtained at the B3LYP/cc-pVDZ level are given in Table 2. The notations used are illustrated in Scheme 2. While going from **3X** to **3X'** (when  $X = O, NH, CH_2, BH, S$ ), the hub ( $r_1$  and  $r_2$ ) and the flank ( $r_3$ ) bond lengths are contracted, whereas the rim bond lengths ( $r_4, r_5, r_6$ ) are elongated. The extent of contraction/elongation while going from bowl to the planar form for all the geometric parameters gradually decreases with the increase in the size of X, with an exception in case of **3PH**, which may be traced to the fact that **3PH'** is not the true transition state corresponding to the bowl-to-bowl inversion process.<sup>41</sup> The contraction of hub bond lengths and the elongation of rim bond lengths are due to the strain energy build up in going from the bowl structure to the flat transition state. In **3NH**, there is a substantial pyramidalization around all N. The minimum energy bowl geometry has  $C_{3v}$  structure where the H's are away from the hub and leaving the lone pairs on the concave face of the bowl. However, the  $D_{3h}$  form was characterized as the true transition state for the bowl-to-bowl inversion. In contrast to the trindenes, the bond lengths in the central six-membered ring of trisubstituted sumanenes are close to the aromatic C–C length in most of the cases. The bond alternation in the hub six-membered ring ( $\Delta_{hub}$ ) is always found to be lower in **3X'** than that in the  $C_{3v}$  (bowl) form, **3X** for all X. In contrast, a substantial increase in the alternation in the rim six-membered ( $\Delta_{rim}$ ) is observed while going from **3X** to **3X'**. This difference is found to gradually decrease with the size of the heteroatom and reverts for **3PH** (i.e.,  $\Delta_{rim}(\mathbf{3PH}) > \Delta_{rim}(\mathbf{3PH}')$ ).  $\Delta_{hub}$  in both **3X** and **3X'** varies with the  $\pi$ -electron count as observed in the case of bond alternation in trindenes (Figure 1).  $\Delta_{hub}$  when  $X = O, NH, S$ , and  $PH$  are lower than that when  $X$

$= CH_2, PH_3, SiH_2$  which are in turn lower when  $X = BH, Si, AlH$ . Even though  $\Delta_{rim}$  of **3X** shows similar variations,  $\Delta_{rim}$  of **3X'** is found to be strain dependent; the smaller the size of the heteroatom the larger the alternation. Thus, in general, in this class of compounds, the bond length alternation in the hub six membered ring is mainly controlled by electronic factors and is independent of the size of the heteroatom.

### 3.2. Bowl Depth, Curvature, and Dipole Moment.

One of the straightforward measures of evaluating the curvature in symmetric buckybowl is the bowl depth (BD), which is the interplanar distance between the two planes formed by the hub and the rim atoms (Scheme 3). The bowl depth seems to be solely controlled by the size of the substituent, which is in agreement with our previous studies (Figure 2).<sup>29,30</sup> Accordingly, a bigger heteroatom placed on the periphery of the bowl flattens it while a smaller atom increases the depth of the bowl. Figure 2 clearly establishes the relationship between the size of the heteroatom and depth of the bowl. Haddon's  $\pi$ -orbital axis vector (POAV) angles have been measured for all the buckybowl using the POAV3 program.<sup>47,48</sup> The bowl depth, POAV angles at the hub, rim-quat, and the rim carbon atoms, and the dipole moment ( $\mu$ ) obtained at the B3LYP/cc-pVDZ level are given in Table 3. The flat structures ( $X = PH_3, Si, SiH_2$ , and  $AlH$ ) have zero bowl depth, no dipole moment, and POAV angles as  $90^\circ$ . With the increase in the size of the heteroatom, decrease in the bowl depth and the POAV angles is seen as evident from Table 3 and Figures 2 and 3. In all the cases as expected, the POAV angle at the hub is greater than that at the rim-quat, which is in turn greater than the POAV angle obtained at the rim position except in **3PH**, which is due to the puckered hydrogen atoms. Dipole moment in buckybowl arises due to their curvature and the presence of heteroatoms. From **3NH** to **3S**, the dipole moment is found to decrease with the bowl depth. **3O** having the maximum bowl depth with interspersed oxygen atoms is expected to show a higher dipole moment, but a lower value of 1.97 D is observed. This is because the dipole due to the oxygen atoms and the dipole arising from the curvature act opposite to each other in this case alone and the direction of the resultant dipole is found to be opposite compared to others. The reason for the higher value of dipole moment of **3PH** is traced to the three heavily puckered hydrogens attached to the P atoms.

**3.3 Inversion Barriers.** A gradual decrease in the bowl-to-bowl inversion barriers ( $\Delta E^\ddagger$ ) with the increase in the size of X is found for the heterosumanenes, **3X** (Table 4).  $\Delta E^\ddagger$  of **3O** and **3NH** are so high that, if synthesized, they are not expected to undergo bowl-to-bowl inversion at room temperature; i.e., they will be locked to a single bowl conformation. However, sumanene, **3CH\_2** is expected to undergo slow inversion near room temperature.<sup>26</sup> Rapid bowl-to-bowl inversion near room temperature for **3BH** and **3S** is evident from their  $\Delta E^\ddagger$  values. The heterosumanenes, **3PH\_3**, **3Si**, **3SiH\_2**, and **3AlH** are no longer bowls, as the planar structures

(47) Haddon, R. C. POAV3: Release 3.0, 1993.

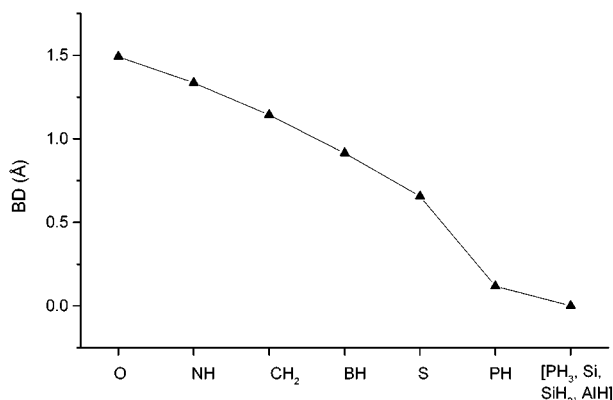
(48) (a) Haddon, R. C. *J. Am. Chem. Soc.* **1990**, *112*, 3385. (b) Haddon, R. C.; Scott, L. T. *Pure Appl. Chem.* **1986**, *58*, 137. (c) Haddon, R. C. *Chem. Phys. Lett.* **1986**, *125*, 231. (d) Haddon, R. C. *J. Am. Chem. Soc.* **1986**, *108*, 2837. (e) Haddon, R. C. *J. Am. Chem. Soc.* **1987**, *109*, 1676. (f) Haddon, R. C. *Acc. Chem. Res.* **1988**, *25*, 243.

(46) C–B bond in **2BH** is unusually short, computed to be 1.535 Å at the B3LYP/cc-pVDZ level.

**Table 2. Principal Geometric Parameters and the Bond Length Alternations in the Hub ( $\Delta_{\text{hub}}$ ) and the Rim ( $\Delta_{\text{rim}}$ ) of the Heterosumanenes (3X and 3X') Obtained at the B3LYP/cc-pVDZ Level**

structure	point group	$r_1$ (Å)	$r_2$ (Å)	$r_3$ (Å)	$r_4$ (Å)	$r_5$ (Å)	$r_6$ (Å)	$\Delta_{\text{hub}}^a$	$\Delta_{\text{rim}}^b$
<b>3O</b>	$C_{3v}$	1.401	1.430	1.392	1.407	1.411	1.419	0.029	0.027
<b>3O'</b>	$D_{3h}$	1.351	1.372	1.354	1.482	1.442	1.476	0.021	0.125
<b>3NH</b>	$C_{3v}$	1.399	1.424	1.402	1.420	1.420	1.417	0.025	0.021
<b>3NH'</b>	$D_{3h}$	1.357	1.377	1.371	1.466	1.445	1.464	0.020	0.107
<b>3CH<sub>2</sub></b>	$C_{3v}$	1.389	1.435	1.402	1.554	1.402	1.433	0.046	0.044
<b>3CH<sub>2</sub>'</b>	$D_{3h}$	1.369	1.401	1.379	1.596	1.420	1.456	0.032	0.087
<b>3BH</b>	$C_{3v}$	1.380	1.442	1.420	1.604	1.404	1.438	0.062	0.058
<b>3BH'</b>	$D_{3h}$	1.369	1.422	1.404	1.635	1.415	1.448	0.053	0.079
<b>3S</b>	$C_{3v}$	1.394	1.416	1.393	1.816	1.413	1.421	0.022	0.028
<b>3S'</b>	$D_{3h}$	1.385	1.405	1.386	1.830	1.417	1.429	0.020	0.044
<b>3PH</b>	$C_{3v}$	1.391	1.426	1.397	1.899	1.407	1.427	0.035	0.036
<b>3PH'</b>	$D_{3h}$	1.397	1.419	1.409	1.797	1.419	1.410	0.022	0.022
<b>3PH<sub>3</sub></b>	$C_{3h}$	1.395	1.436	1.392	1.879	1.401	1.427	0.041	0.035
				(1.394)	(2.098)	(1.406)			
<b>3Si</b>	$D_{3h}$	1.388	1.438	1.415	1.971	1.404	1.431	0.050	0.043
<b>3SiH<sub>2</sub></b>	$D_{3h}$	1.399	1.449	1.413	1.917	1.400	1.421	0.050	0.022
<b>3AlH</b>	$D_{3h}$	1.407	1.470	1.429	1.971	1.396	1.415	0.063	0.033

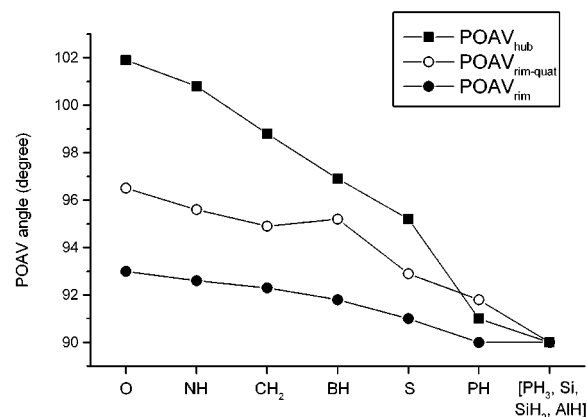
<sup>a</sup>  $\Delta_{\text{hub}} = r_2 - r_1$  is the bond length alternation in the hub six-membered ring. <sup>b</sup>  $\Delta_{\text{rim}}$  is the maximum bond alternation in the rim six-membered ring.

**Figure 2.** Variation of bowl depth (BD) of the heterosumanenes (3X) obtained at the B3LYP/cc-pVDZ level.**Scheme 3****Table 3. Bowl Depth, BD (Å), and POAV Angles (Deg) at the Hub, Rim-Quat, and Rim Carbons (POAV<sub>hub</sub>, POAV<sub>rim-quat</sub>, and POAV<sub>rim</sub>, Respectively) and the Dipole Moment ( $\mu$  in Debye) for the Heterosumanenes (3X) Obtained at the B3LYP/cc-pVDZ Level**

structure <sup>a</sup>	BD (Å)	POAV <sub>hub</sub>	POAV <sub>rim-quat</sub>	POAV <sub>rim</sub>	$\mu$ (D)
<b>3O</b>	1.492	101.9	96.5	93.0	1.97
<b>3NH</b>	1.336	100.8	95.6	92.6	4.88
<b>3CH<sub>2</sub></b>	1.143	98.8	94.9	92.3	2.10
<b>3BH</b>	0.914	96.9	95.2	91.8	1.27
<b>3S</b>	0.656	95.2	92.9	91.0	1.03
<b>3PH</b>	0.118	91.0	91.8	90.0	1.33

<sup>a</sup> For **3PH<sub>3</sub>**, **3Si**, **3SiH<sub>2</sub>**, and **3AlH**, the planar structure is the minimum, so the bowl depth will be zero and the POAV angles will be 90°.

correspond to minima on the respective potential energy surfaces. The flat  $D_{3h}$  structure of **3PH** has been characterized as a third-order saddle point, and the normal modes of the three imaginary frequencies correspond to the pyramidal inversion at the three phosphorus atoms. Since none of the normal modes corresponding to the imaginary frequencies represent the transition state for the bowl-to-bowl inversion, **3PH** also does not undergo inversion.<sup>41</sup> However, the skeleton

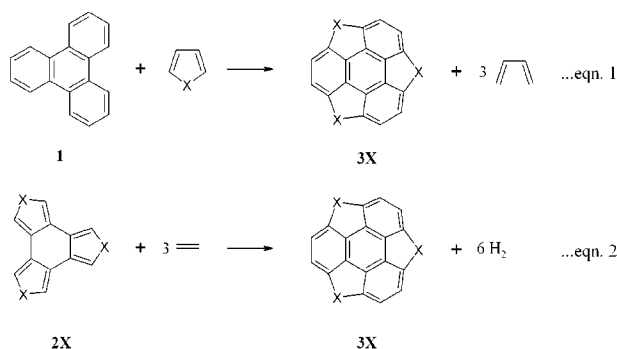
**Figure 3.** Plot of the POAV angles at the hub, rim-quat, and rim carbons of the heterosumanenes (3X) computed at the B3LYP/cc-pVDZ level of theory.**Table 4. Bowl-to-Bowl Inversion Barrier,  $\Delta E^\ddagger$  (in kcal/mol), Enthalpy of Activation,  $\Delta H^\ddagger$  (in kcal/mol), Reaction Energies,  $\Delta E(1)$  and  $\Delta E(2)$  of Reactions 1 and 2 (in kcal/mol), and Chemical Hardness,  $\eta$  (in eV), of the Heterosumanenes (3X) Obtained at the B3LYP/cc-pVDZ Level**

X	$\Delta E^\ddagger$ (kcal/mol)	$\Delta H^\ddagger$ (kcal/mol)	$\Delta E(1)$ (kcal/mol)	$\Delta E(2)$ (kcal/mol)	$\eta$ (eV)
<b>3O</b>	69.6	68.3	130.0	80.7	2.14
<b>3NH</b>	44.1	43.3	125.6	78.0	1.99
<b>3CH<sub>2</sub></b>	18.2	17.5	63.3	20.3	2.35
<b>3BH</b>	6.6	6.0	10.7	-22.3	1.33
<b>3S</b>	1.9	1.6	76.4	29.8	2.13
<b>3PH<sup>a</sup></b>			35.3	-9.1	2.30
<b>3PH<sub>3</sub></b>	<i>b</i>	<i>b</i>	15.2	-26.6	2.19
<b>3Si</b>	<i>b</i>	<i>b</i>	-8.0	-45.1	1.11
<b>3SiH<sub>2</sub></b>	<i>b</i>	<i>b</i>	7.1	-38.6	2.16
<b>3AlH</b>	<i>b</i>	<i>b</i>	-8.0	-56.6	1.65

<sup>a</sup> The energy difference between the  $C_{3v}$  and  $D_{3h}$  structures is 85.6 kcal/mol, which in this case does not correspond to the inversion barrier. <sup>b</sup> The equilibrium structure is flat.

(devoid of hydrogens) of the  $C_{3v}$  structure of **3PH**, which is characterized as a minimum, is virtually flat with the hydrogens connected to the three phosphorus atoms heavily puckered. Therefore, the bowl-to-bowl inversion barrier seems to be exclusively controlled by the size of the substituent and independent of any electronic factors.

Scheme 4



**3.4 Stability of the Heterosumanenes.** The thermodynamic stability of the heterosumanenes **3X** are assessed using the homodesmotic eqs 1 and 2 given in Scheme 4; the corresponding reaction energies  $\Delta E(1)$  and  $\Delta E(2)$  obtained at the B3LYP/cc-pVDZ level are given in Table 4. Although the ordering of the thermodynamic stabilities are very similar in both cases, eq 2, where trindene (**2CH<sub>2</sub>**) is taken as reference uniformly gives higher stability compared to eq 1 where triphenylene (**1**) is taken as reference. The stability as such seems to be controlled by two factors, namely the size of the heteroatom and the total  $\pi$ -electron count of the buckybowl. A general feature is that the thermodynamic stability increases as the size of the heteroatom increases, simply due to the favorable strain energy. However,  $24\pi$ -systems ( $X = \text{O}, \text{S}, \text{NH}$ , and  $\text{PH}$ ) exhibit lower stability partly because of the way the homodesmotic equations are set up. Since these two factors compete in deciding the stability, direct correlation between the thermodynamic stability is not possible when taking the  $18\pi$  and  $24\pi$  electron systems together. However, within a given  $\pi$ -electron count the size of the heteroatom exclusively controls the thermodynamic stability of the heterobowls, a result which is consistent with previous observations.<sup>29–31</sup> Compared to sumanene, only **3O**, **3NH**, and **3S** are found to be unstable. **3S**, which is computed to be less stable than sumanene and most other heterosumanenes, has been synthesized recently.<sup>23</sup>

Chemical hardness ( $\eta$ ), which may be defined as  $\eta = (E_{\text{LUMO}} - E_{\text{HOMO}})/2$ , within the Koopman's approximation, was found to be a good measure of the stability of the system.<sup>49</sup> The measured  $\eta$  values for all the heterosumanenes (**3X**) considered here are given in Table 4. Surprisingly, sumanene (**3CH<sub>2</sub>**) was computed to be the hardest of all the considered, and so it is the most stable in that sense. This analysis also indicates that  $\eta$  values are too low for  $X = \text{BH}$ ,  $\text{Si}$ , and  $\text{AlH}$ , indicating that these compounds will be very reactive and might provide severe challenges to synthetic attempts. Thus,  $\eta$  indicates that  $18\pi$ -systems with fully extended  $\pi$ -framework are less stable and the stability of the rest are comparable. Both the homodesmotic equations and chemical hardness analysis point that this class of compounds is fairly stable and synthetic attempts toward these compounds should be rewarding.

### 3.5. Structure–Inversion Barrier Relationship.

The importance of structure–energy correlations in elucidating the reaction mechanisms was recognized long time back.<sup>27</sup> Burgi and Dubler-Steudle, in a ring-inversion study, showed that a quartic function fits the activation energy of a ring inversion and the distortion from the planarity in a series of metallocyclopentenes.<sup>27a</sup>

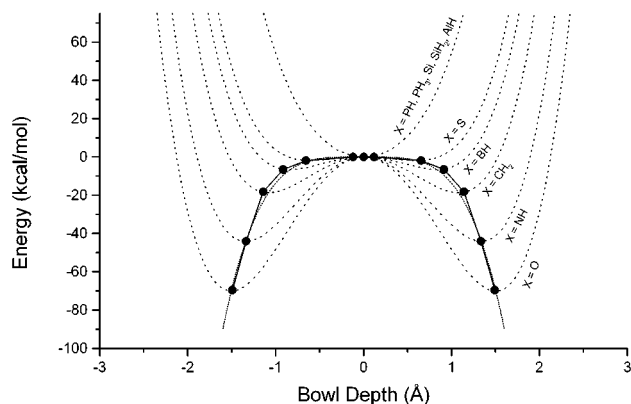


**Figure 4.** Plot showing the correlation of bowl depth and the bowl-to-bowl inversion barrier (shown in thick dotted lines). Thin dotted lines correspond to the empirical double-well potentials for the bowl structures and single-well potential for the flat minima. The thick dotted line is fit with a quartic function and the dotted lines by a mixed quartic/quadratic function. The continuous line corresponds to the computed results.

Siegel et al. have tested that the quartic function excellently fits the experimentally (or computationally) determined inversion barrier, for a series of substituted corannulenes, and their bowl depth.<sup>28</sup>

However, Burgi and Siegel et al. have shown that a closer analysis reveals that there is an attractive and repulsive part which results in a double well potential.<sup>27,28</sup> The double-well potential is nothing but a function of  $x$ , which is a quartic minus quadratic type as given in eq 1.

$$E = ax^4 - bx^2 \quad (3)$$

At the equilibrium geometry of the bowl structure, i.e., at the minima, the first derivative of energy with respect to the reaction coordinate should vanish,  $(\Delta E/\Delta x) = 0$ .

Therefore,

$$4ax^3 - 2bx = 0 \quad (4)$$

Solving eq 2, we get

$$x = 0; x^2 = b/2a \Rightarrow b = 2ax_{\text{eq}}^2 \quad (5)$$

$$-\Delta E^\ddagger = E(x_{\text{eq}}) - E(x_0)$$

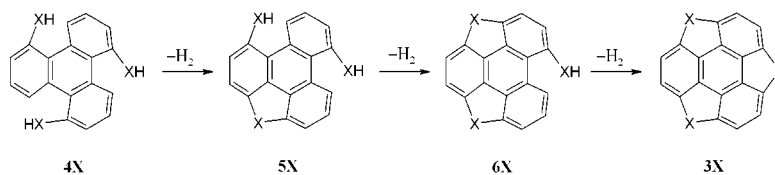
$x_{\text{eq}}$  is the bowl depth at the minima and  $x_0$  is that in the transition state, which is zero.

$$-\Delta E^\ddagger = (ax_{\text{eq}}^4 - 2ax_{\text{eq}}^2x_{\text{eq}}^2) - 0 = -ax_{\text{eq}}^4 \quad (6)$$

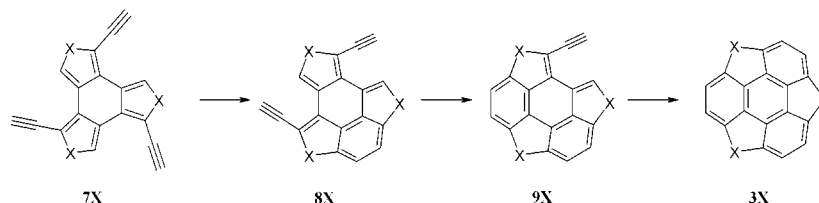
So, a quartic function nicely correlates the bowl-to-bowl inversion barrier and the bowl depth in this class of compounds (eq 6), as shown in Figure 4. Figure 4 reveals that at higher bowl depths the potential is much steeper, and in contrast, the potential is much softer at smaller bowl depths, similar to Siegel's structure–energy correlations of substituted corannulenes.<sup>28</sup> Therefore, small perturbations either in solvent or steric effect by adding bulky groups, for the flat minima and bowls with smaller curvature should lead to substantial changes in the geometry. However higher levels of perturbation are required to change the shape and bowl depth for the

## Scheme 5

(a) Triphenylene Route:



(b) Trindene Route:



deeper bowls. The single-well potential observed for **3X**,  $X = \text{PH}, \text{PH}_3, \text{Si}, \text{SiH}_2$ , and  $\text{AlH}$ , indicates that the energy increases along the bowl inversion mode when  $x$  deviates from zero. Of course, the shape of the single well depends on the nature of substituent, and only an idealized picture is given in Figure 4. These single-well and double-well potentials are reminiscent of the situation in the pyramidal inversion of  $\text{BH}_3$  and  $\text{NH}_3$  respectively.

Transition metal complexation to fullerenes is restricted mostly to  $\eta^2$  type;  $\eta^5$  and  $\eta^6$  coordinations are rare.<sup>50</sup> Fullerenes, with their splayed orbitals rendering reduced overlap, will be unfavorable due to their rigid geometry in terms of orbital compatibility.<sup>51</sup> Also due to the inherent rigidity of fullerenes, they do not leave much scope for chemical manipulations. In contrast, the heterobuckybowls, with their flexible geometry provides much scope for  $\eta^6$  complexations either with the hub or the rim benzenoid rings.

**3.6. Synthetic Strategies: Triphenylene versus Trindene Route.** Ring closure strategies starting from a suitably functionalized hydrocarbon skeleton were found to be the most successful synthetic strategies for buckybowl. We conceived two idealized  $C_3$ -symmetric pathways, namely a triphenylene route and a trindene route, which could target the buckybowl in a sequential ring-closure process (Scheme 5).

The reaction energies of the dehydrogenations (triphenylene route)  $4\text{X} \rightarrow 5\text{X} \rightarrow 6\text{X} \rightarrow 3\text{X}$  and the reaction energies of the isomerization reactions (trindene route)  $7\text{X} \rightarrow 8\text{X} \rightarrow 9\text{X} \rightarrow 3\text{X}$  were calculated (Scheme 5) using the B3LYP/cc-pVDZ single-point calculations done on the corresponding MNDO equilibrium geometries. The reaction energies obtained via the triphenylene and the trindene routes are plotted against the number of bridges and given in Figures 5 and 6, respectively. Along the triphenylene route, the strain buildup increases and the third bridging becomes crucial, and hence, the synthesis of both **3CH<sub>2</sub>** and **3S** could not be achieved through this

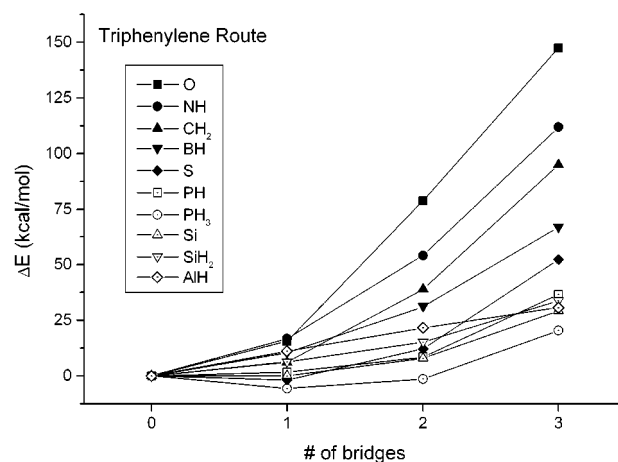


**Figure 5.** Reaction energies (Scheme 5a), which correspond to the strain energy buildup, obtained for the sequential ring closing to form heterosumanenes (**3X**) via the triphenylene route.

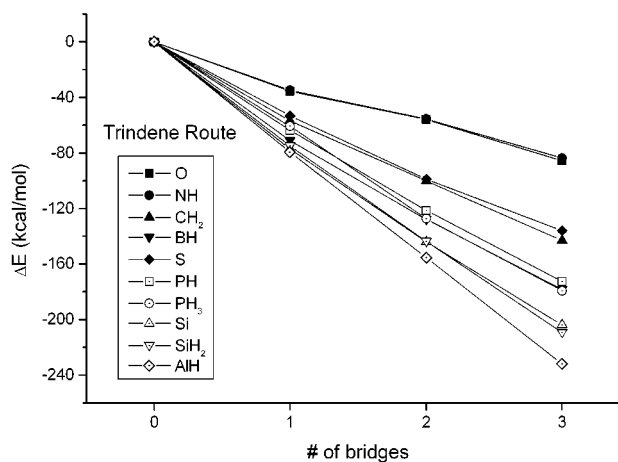


**Figure 6.** Reaction energies (Scheme 5b), which correspond to the strain energy buildup, obtained for the sequential ring closing to form heterosumanenes (**3X**) via the trindene route.

route.<sup>25,53</sup> The energy difference decreases with the increasing size of the atom, and the strain buildup in each step when  $X = \text{PH}, \text{Si}, \text{SiH}_2$ , and  $\text{AlH}$  indicates that the synthesis of these compounds might be achieved by

(49) (a) Pearson, R. G. *J. Org. Chem.* **1989**, *54*, 1423. (b) Zhou, Z.; Parr, R. G. *Tetrahedron Lett.* **1988**, *29*, 4843. (c) Zhou, Z.; Parr, R. G. *J. Am. Chem. Soc.* **1989**, *111*, 7371. (d) Minsky, A.; Meyer, A. Y.; Rabinovitz, M. *Tetrahedron* **1985**, *41*, 785. (e) Pearson, R. G. *J. Am. Chem. Soc.* **1988**, *110*, 2092.

(50) Jemmis, E. D.; Manoharan, M.; Sharma, P. K. *Organometallics* **2000**, *19*, 1879.

(51) Jemmis, E. D. *J. Am. Chem. Soc.* **1982**, *104*, 7017.

following the triphenylene route itself. Along the trindene route, all the reaction energies are negative, indicating the feasibility of the formation of **3X**. Figures 5 and 6 indicate that as the size of the heteroatom increases, the strain energy buildup becomes uniform in both triphenylene and trindene routes. A closer look at Figures 5 and 6 also indicates that  $18\pi$  systems are much more facile than the  $24\pi$  system. But, it is to be noted that the synthesis of suitably functionalized precursors is the key in all these cases and our computational results ensure that once a trindene precursor is prepared, effecting the sequential ring closures is easier. So, the syntheses of **3X** may be achieved once the precursors for the trindene route are achieved. Our theoretical studies<sup>31,52</sup> clearly account for the success of Otsubo et al.<sup>23</sup> in the synthesis of trithiasumanene, **3S** in the trindene route. Similarly, the failure to achieve the final ring-closure step for **3S**, by Klemm et al.,<sup>53</sup> and **3CH<sub>2</sub>**, by Mehta et al.,<sup>25</sup> are obvious from the above analysis.

#### 4. Conclusions

A systematic computational study of the hitherto less explored heterobuckybowls has revealed the interrelationship among the bowl depth, inversion barrier, and synthetic feasibility. The bowl depth and the bowl-to-bowl inversion barrier were found to be largely controlled by the size of the heteroatom. Significant variations in the bond alternations as a function of substituents are observed; the bond length alternation computed in **2BH** was found to match with the highest value reported for benzenoid rings.<sup>34d,e</sup> While the bowl depth and inversion barrier depends on the size of the substituent and the concomitant strain energy buildup in the polycyclic skeleton, the bond alternation is controlled mainly by the electronic factors.

(52) (a) Jemmis, E. D.; Sastry, G. N.; Mehta, G. *J. Chem. Soc., Perkin Trans. 2* **1994**, 437. (b) Dinadayalane, T. C.; Sastry, G. N. *Tetrahedron Lett.* **2001**, 42, 6421.

(53) Klemm, L. H.; Hall, E.; Cousins, L.; Klopfenstein, C. E. *J. Heterocycl. Chem.* **1989**, 26, 345.

(54) Hedberg, L.; Hedberg, K.; Cheng, P.-C.; Scott, L. T. *J. Phys. Chem. A* **2000**, 104, 7689.

The energy profile of the heterobuckybowls was fit to a double-well potential, which results in an empirical correlation between the bowl-to-bowl inversion and the bowl depth, which parallels the structure/energy correlations of Burgi<sup>27</sup> and discussed recently by Siegel et al., in substituted corannulenes.<sup>28</sup> The differences in the bowl-to-bowl inversion barriers nicely correspond to the perturbations in the strain energy of the reference flat structure, which in turn seems to be controlled exclusively by the size of the heteroatom. Thermodynamically, most of these yet unknown heterobowls are found to be more stable than the already synthesized trithiasumanene (**3S**), and this should encourage experimental studies directed toward this fascinating class of compounds.<sup>23</sup> Additionally, the chemical hardness which gauges the reactivity does not show very low values, indicating that these compounds, if synthesized, should show reasonable kinetic stability. Suitable synthetic strategies delineated in the present study should make this very promising class of compounds accessible. The present study unequivocally proves that larger heteroatom substituents on the periphery leads to flat structures with reduced bowl-to-bowl inversion barriers, and the ring-closure strategy to synthesize the bowl shaped molecules would greatly benefit by larger heteroatom substitutions.

**Acknowledgment.** CSIR (No.01(1681)/00/EMRII) is thanked for the financial assistance. We thank the staff of the Department of Organic Chemistry (Indian Institute of Science) for their kind hospitality and support and SERC for extending computational facilities. U.D.P. thanks UGC, New Delhi, for a Junior Research Fellowship.

**Supporting Information Available:** Tables of Cartesian coordinates of B3LYP/cc-pVDZ-optimized minimum energy bowl geometries, the transition states for the inversion and the trindenenes, and figures of the simulated vibrational spectra for all the equilibrium structures considered in the study. Tables of total energies of all the structures in the synthetic routes at the B3LYP/cc-pVDZ//MNDO level. This material is available free of charge via the Internet at <http://pubs.acs.org>.

JO015775K